

Two ferromagnetic phases with different spin states of Mn and Ni in $\text{LaMn}_{0.5}\text{Ni}_{0.5}\text{O}_3$

V. L. Joseph Joly, P. A. Joy,* and S. K. Date

Physical and Materials Chemistry Division, National Chemical Laboratory, Pune 411008, India

C. S. Gopinath

Catalysis Division, National Chemical Laboratory, Pune 411008, India

(Received 15 December 2001; revised manuscript received 1 March 2002; published 24 April 2002)

A ferromagnetic transition below 280 K is observed in the temperature variation of the magnetization, measured using high magnetic fields, for samples of $\text{LaMn}_{0.5}\text{Ni}_{0.5}\text{O}_3$ synthesized by the high-temperature solid-state reaction method. On the other hand, two well-defined magnetic transitions, at ~ 150 and ~ 280 K, are observed in low-field zero-field-cooled (ZFC) magnetization (M_{ZFC}) measurements on these samples, indicating the possibility for the existence of two different ferromagnetic phases of the compound. $\text{LaMn}_{0.5}\text{Ni}_{0.5}\text{O}_3$, synthesized by a low-temperature method, shows a single magnetic transition at ~ 150 K for samples annealed below 500°C and a single magnetic transition at 280 K for samples annealed above 1000°C in the low-field M_{ZFC} measurements. Broad or multiple magnetic transitions are observed for the low-temperature samples annealed in the temperature range $500\text{--}1000^\circ\text{C}$. High-temperature magnetic susceptibility, powder x-ray-diffraction, and core-level x-ray photoelectron spectroscopic studies on the single-phase samples (annealed at 400 and 1300°C) indicate that the nanocrystalline material (obtained at 400°C) with spin states of Mn and Ni as Mn^{4+} and Ni^{2+} undergoes a magnetic transition below 150 K, whereas high temperature (1300°C) annealed material with spin states like Mn^{3+} and low-spin Ni^{3+} becomes ferromagnetic below 280 K. A charge disproportionation of the type $\text{Mn}^{4+} + \text{Ni}^{2+} \rightarrow \text{Mn}^{3+} + \text{Ni}^{3+}$ takes place when the low-temperature synthesized $\text{LaMn}_{0.5}\text{Ni}_{0.5}\text{O}_3$ is annealed above 500°C . The results give evidence for the existence of two different phases of $\text{LaMn}_{0.5}\text{Ni}_{0.5}\text{O}_3$ with different crystal structures and different spin states of Mn and Ni.

DOI: 10.1103/PhysRevB.65.184416

PACS number(s): 75.30.-m, 75.50.-y, 81.40.Rs, 82.30.Hk

I. INTRODUCTION

Recent interest in the study of the double perovskites $A_2BB'O_6$ stems from the observation of large tunnelling magnetoresistance at room temperature in the half-metallic compound $\text{Sr}_2\text{FeMoO}_6$.¹ $\text{Sr}_2\text{FeMoO}_6$ is a ferromagnet at room temperature, and is a promising candidate for devices based on intergrain-tunnelling magnetoresistance. Two different crystallographic forms with different Curie temperatures are reported for $\text{Sr}_2\text{FeMoO}_6$: a cubic phase with $T_c = 390$ K and a tetragonal phase with $T_c = 415$ K.¹⁻³ The Fe and Mo ions in $\text{Sr}_2\text{FeMoO}_6$ are found to be mixed valent, from paramagnetic susceptibility and Mössbauer spectroscopic studies, and the majority of the ions are present as Fe^{3+} and Mo^{5+} .^{4,5} It has been predicted that the perfect alternating order of Fe and Mo ions in the octahedral sites promotes the equilibrium $\text{Fe}^{3+} + \text{Mo}^{5+} \leftrightarrow \text{Fe}^{2+} + \text{Mo}^{6+}$, and that the overlapping of the redox energies of $\text{Fe}^{3+}/\text{Fe}^{2+}$ and $\text{Mo}^{6+}/\text{Mo}^{5+}$ pairs give rise to half-metallicity and ferromagnetism in $\text{Sr}_2\text{FeMoO}_6$.^{3,6}

The mixed valency of transition-metal ions, the charge disproportionation, the existence of two different crystallographic forms, etc., appear to be some of the common features of the perovskite type magnetic oxides $A_2BB'O_6$ ($AB_{0.5}B'_{0.5}O_3$).⁷⁻¹⁰ The magnetic properties of the manganese oxides La_2MnMO_6 , where $M = \text{Co}, \text{Ni}, \text{Cr}$, etc., were first studied in the 1960s (both the perovskite formula $\text{LaMn}_{0.5}M_{0.5}\text{O}_3$ and the double perovskite formula La_2MnMO_6 were commonly used by the earlier workers), to

understand the nature of the magnetic exchange interactions in these compounds.¹¹⁻¹⁶ When $M = \text{Co}$ or Ni , the compounds were found to order ferromagnetically, compared to the antiferromagnetic, diamagnetic, and paramagnetic behaviors of LaMnO_3 , LaCoO_3 , and LaNiO_3 , respectively. Stoichiometric LaMnO_3 has an orthorhombic perovskite structure, whereas LaCoO_3 and LaNiO_3 are rhombohedral.¹⁷ Because of the different structures of the end members, it is possible that La_2MnMO_6 may form in two different structures. Goodenough *et al.*¹² observed two different ferromagnetic Curie temperatures for $\text{LaMn}_{0.5}\text{Co}_{0.5}\text{O}_3$, due to the presence of orthorhombic and rhombohedral phases of the compound in their samples synthesized by the conventional solid-state reaction method. Goodenough and co-workers were of the opinion that the Mn ions are trivalent in these compounds with the M ions Co and Ni in their trivalent low-spin states so that ferromagnetism in these compounds is due to $\text{Mn}^{3+}\text{-O-Mn}^{3+}$ superexchange interactions.^{11,12} Their attempts to synthesize ordered $\text{LaMn}_{0.5}^{4+}M_{0.5}^{2+}\text{O}_3$ were not successful, and found that the cations favor $\text{LaMn}_{0.5}^{3+}\text{Co}_{0.5}^{\text{III}}\text{O}_3$ and $\text{LaMn}_{0.5}^{3+}\text{Ni}_{0.5}^{\text{III}}\text{O}_3$ (the notation M^{III} is commonly used to represent low-spin trivalent ions) so that there is no ordering on the B sublattice. Jonker,¹⁴ however, concluded that a mixture of Mn^{3+} and Co^{3+} ions, as in LaMnO_3 and LaCoO_3 , tend to form $\text{Mn}^{4+}\text{-Co}^{2+}$ pairs in $\text{LaMn}_{0.5}\text{Co}_{0.5}\text{O}_3$ due to the charge disproportionation $\text{Mn}^{3+} + \text{Co}^{3+} \rightarrow \text{Mn}^{4+} + \text{Co}^{2+}$. On the other hand, Vasanthacharya *et al.*¹⁸ showed that the reverse reaction $\text{Mn}^{4+} + \text{Ni}^{2+} \rightarrow \text{Mn}^{3+} + \text{Ni}^{3+}$ is favored in the case of $\text{LaMn}_{0.5}\text{Ni}_{0.5}\text{O}_3$. Other magnetic^{13,15} and ⁵⁵Mn NMR (Ref. 19-21) studies also gave evidence for the $\text{Mn}^{4+}\text{-O-M}^{2+}$ superexchange interactions in La_2MnMO_6 .

Recently, we have prepared two different ferromagnetic phases of $\text{LaMn}_{0.5}\text{Co}_{0.5}\text{O}_3$, in single-phase forms, by a low-temperature method of synthesis.²² The material obtained by the conventional solid-state reaction method was found to be a mixture of the two different phases of the compound. The rhombohedral phase of $\text{LaMn}_{0.5}\text{Co}_{0.5}\text{O}_3$ in single-phase form is found to be stable only below 700 °C, and the second phase in single phase form is obtained only after heating at 1300 °C. The rhombohedral phase orders ferromagnetically at a higher Curie temperature when compared to the lower magnetic ordering temperature of the orthorhombic phase. Apart from the difference in the structures and Curie temperatures, the major difference between the two phases was found to be the difference in the nature of the magnetic exchange interactions because of the different spin states of Mn and Co in the two different phases of the compound.^{23,24} Mn and Co ions were found to be present as Mn^{3+} and low-spin Co^{3+} in the high- T_c , rhombohedral, phase, so that ferromagnetism is due to $\text{Mn}^{3+}\text{-O-Mn}^{3+}$ superexchange interactions. On the other hand, the low- T_c , orthorhombic, phase consists of Mn^{4+} and Co^{2+} , so that $\text{Mn}^{4+}\text{-O-Co}^{2+}$ superexchange interactions are responsible for ferromagnetism in this phase of the compound. The rhombohedral phase of the compound is slowly converted to the orthorhombic phase when heated above 700 °C, accompanied by the charge disproportionation $\text{Mn}^{3+} + \text{Co}^{3+} \rightarrow \text{Mn}^{4+} + \text{Co}^{2+}$. Therefore, the material synthesized by the conventional ceramic method always contains mixed phases of $\text{LaMn}_{0.5}\text{Co}_{0.5}\text{O}_3$ in different amounts and mixed valence states of Mn and Co when samples are prepared after heating in the temperature range 1000–1300 °C which is the processing temperature range adopted for the synthesis of substituted perovskite type oxides.

One of the interesting properties observed for $\text{LaMn}_{0.5}\text{Co}_{0.5}\text{O}_3$ is its unusual magnetic behavior when the material is in the nanocrystalline form.²⁵ Nanocrystalline $\text{LaMn}_{0.5}\text{Co}_{0.5}\text{O}_3$ is found to possess magnetic properties similar to that observed for the phase obtained at higher processing temperatures having a lower T_c . Thus an unusual charge disproportionation of the type $\text{Mn}^{4+} + \text{Co}^{2+} \rightarrow \text{Mn}^{3+} + \text{Co}^{3+} \rightarrow \text{Mn}^{4+} + \text{Co}^{2+}$ was found to be operative in nanocrystalline $\text{LaMn}_{0.5}\text{Co}_{0.5}\text{O}_3$, when samples were annealed in air in the temperature range 200–1300 °C.²⁵ The low- T_c phase of the compound formed initially at very low temperatures is transformed to the high- T_c phase and then again converted back to the low- T_c phase when annealed in this temperature range due to the above charge disproportionation.

In stoichiometric LaMnO_3 with a GdFeO_3 -type orthorhombic structure, ferromagnetic layers of Mn^{3+} ions are coupled antiferromagnetically, giving rise to A-type layered antiferromagnetic ordering and very weak ferromagnetism at low temperatures due to a canted antiferromagnetic arrangement of spins.²⁶ However, high-temperature susceptibility measurements above the orthorhombic-cubic transition temperature give large positive value for the paramagnetic Curie temperature, indicating the possibility of ferromagnetism in the cubic phase of the compound.^{14,27} This unusual magnetic behavior of LaMnO_3 is due to the Jahn-Teller (JT) distortion

of Mn^{3+} ion.²⁸ The cubic form of the compound at high temperatures is orthorhombically distorted below a certain temperature because of the JT distortion. Substitution of part of Mn^{3+} in LaMnO_3 by other trivalent ions induces ferromagnetism due to the decreased JT distortion, as in $\text{LaMn}_{1-x}\text{Ga}_x\text{O}_3$ and $\text{LaMn}_{1-x}\text{Co}_x\text{O}_3$ containing diamagnetic, low-spin ($S=0$), Co^{3+} ions.¹² If the diamagnetic low-spin Co^{3+} ion in $\text{LaMn}_{0.5}\text{Co}_{0.5}\text{O}_3$ is replaced by low-spin Ni^{3+} ($S=1/2$), the magnetic properties are expected to change considerably. This is because, low-spin Ni^{3+} is a Jahn-Teller ion similar to Mn^{3+} , having one unpaired electron in the e_g orbital. The combined JT distortion of Mn^{3+} and low-spin Ni^{3+} is thus expected to alter the magnetic properties of $\text{LaMn}_{0.5}\text{Ni}_{0.5}\text{O}_3$ drastically. In fact, a higher $T_c=280$ K has been reported for $\text{LaMn}_{0.5}\text{Ni}_{0.5}\text{O}_3$ when compared to the $T_c=230$ K for $\text{LaMn}_{0.5}\text{Co}_{0.5}\text{O}_3$,¹² despite the very small size difference between low-spin trivalent Co (0.545 Å) and Ni (0.56 Å) ions. Goodenough *et al.*¹² attributed this to the combined effect of positive $\text{Mn}^{3+}\text{-O-Mn}^{3+}$ and $\text{Mn}^{3+}\text{-O-Ni}^{3+}$ (Ni^{3+} in the low-spin state) superexchange interactions. Wold *et al.*¹¹ also found that their samples synthesized by the ceramic method, containing less than 2% Ni^{2+} , is orthorhombic with Mn^{3+} and low-spin Ni^{3+} . On the other hand, Blasse argued that ferromagnetism in $\text{LaMn}_{0.5}\text{Ni}_{0.5}\text{O}_3$ is entirely due to $\text{Mn}^{4+}\text{-O-Ni}^{2+}$ superexchange interactions,¹³ which was later concluded²⁰ from ⁵⁵Mn NMR linewidth measurements. However, Sonobe and Asai found that the x-ray-diffraction patterns of their samples, synthesized by the usual solid-state reaction of the corresponding oxides and low-temperature methods, were a superposition of the patterns of a major orthorhombic phase and minor amounts of a rhombohedral phase.²⁰ The fraction of the orthorhombic phase content increased with annealing in oxygen. This implies that $\text{LaMn}_{0.5}\text{Ni}_{0.5}\text{O}_3$ also may form in two different crystallographic modifications, as expected from the different crystal structures of the end members LaMnO_3 and LaNiO_3 , which may coexist in the samples processed in a certain temperature range, as found for $\text{LaMn}_{0.5}\text{Co}_{0.5}\text{O}_3$. However, there is no report so far in the literature on the existence of two ferromagnetic phases of $\text{LaMn}_{0.5}\text{Ni}_{0.5}\text{O}_3$.

In view of the report on the the coexistence of two crystallographic forms of $\text{LaMn}_{0.5}\text{Ni}_{0.5}\text{O}_3$ by Sonobe and Asai,²⁰ the mixed-phase behavior observed for $\text{LaMn}_{0.5}\text{Co}_{0.5}\text{O}_3$ samples synthesized by the solid-state reaction method and the different spin states of Mn and Co in the two different single phase forms,^{22–24} and the observation of an unusual charge disproportionation in the nanocrystalline form of $\text{LaMn}_{0.5}\text{Co}_{0.5}\text{O}_3$ synthesized by a low-temperature method,²⁵ we have synthesized $\text{LaMn}_{0.5}\text{Ni}_{0.5}\text{O}_3$ by the usual ceramic and low-temperature methods, and studied the magnetic properties of the samples heated to different temperatures. The studies were aimed at resolving the problem of the spin states of Mn and Ni, and therefore, to verify the nature of the magnetic exchange interactions in $\text{LaMn}_{0.5}\text{Ni}_{0.5}\text{O}_3$. The existence of two ferromagnetic phases of $\text{LaMn}_{0.5}\text{Ni}_{0.5}\text{O}_3$ with different spin states of Mn and Ni has been identified in the

present work, from magnetic and core-level x-ray photoelectron spectroscopic studies.

II. EXPERIMENT

$\text{LaMn}_{0.5}\text{Ni}_{0.5}\text{O}_3$ (LMN) samples were synthesized by the conventional high-temperature (referred as HT samples in the text) solid-state reaction (ceramic) method and a low-temperature (referred as LT samples in the text) method. In the ceramic method, a stoichiometric mixture of La_2O_3 , MnO_2 and NiO was heated at 1000°C for two days with two intermediate grindings. The powders obtained were then heated at 1100 and 1200°C for one day each and then at 1300°C for four days with intermediate grindings. All the heatings were made in air and the samples were then furnace cooled to room temperature. $\text{LaMn}_{0.5}\text{Ni}_{0.5}\text{O}_3$ and a sample of $\text{NdMn}_{0.5}\text{Ni}_{0.5}\text{O}_3$ were prepared by a low-temperature glycine-nitrate method,²⁹ as described previously.²² In the low-temperature method, the powder samples obtained after initial decomposition of a metal nitrate-glycine mixture at $\sim 200^\circ\text{C}$ was then heated at different temperatures in the range 200 – 1300°C for 12 h each in air, and furnace cooled to room temperature.

Powder x-ray diffraction (XRD) patterns were recorded on a Philips PW 1830 powder x-ray diffractometer. Magnetic measurements were performed on a PAR EG&G vibrating sample magnetometer. The temperature variation of the magnetization (80 – 300 K) was measured after cooling the samples in zero magnetic field [zero-field-cooled (ZFC), magnetization] and then recording the magnetization while warming the sample in a field of 50 Oe. ZFC magnetization curves were recorded on all samples after heating at a given temperature. Photoemission spectra at room temperature were recorded on a VG Microtech Multilab ESCA 3000 spectrometer using $\text{Mg } K\alpha$ x-ray source (1253.6 eV), as described previously.²⁴ Extreme care has been taken to minimize the surface contamination problem by scraping the samples thoroughly and repeatedly over the surface with a stainless steel blade *in situ* under high vacuum. The scraping was repeated until the higher binding energy shoulder in the $\text{O } 1s$ X-ray photoemission spectroscopy (XPS) showed a minimum and no further decrease in intensity. In the case of the LT samples heated at 400°C , on which XPS measurements were made, excess carbon was found in the samples. Perovskite manganites synthesized by the low-temperature methods are known for carbon contamination.^{29,30} Repeated scraping of the samples did not remove the carbon contamination in the LT samples, indicating the presence of carbon in the bulk. However, very good improvement in the spectral quality of $\text{O } 1s$, $\text{C } 1s$, and valence-band spectra of the LT samples after scraping clearly indicated that the bulk carbon contamination do not significantly affect the overall results presented here. Further, core-level XPS measurements were made on three different LT samples, each to make sure that the results are reproducible. Oxygen stoichiometry was determined by redox titration, using potassium permanganate and ferrous sulphate. The oxygen stoichiometry of the sample heated at 1300°C was found to be 3 ± 0.01 . The sample heated at 400°C was found to be slightly oxygen

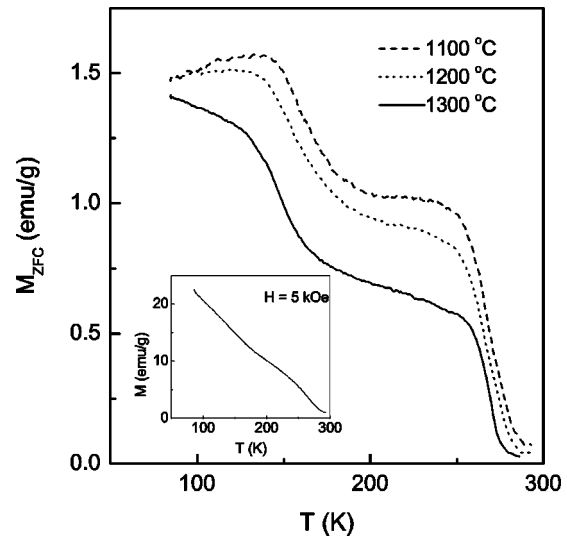


FIG. 1. ZFC magnetization curves ($H = 50$ Oe) of the ceramic (HT) $\text{LaMn}_{0.5}\text{Ni}_{0.5}\text{O}_3$ samples annealed at 1100 , 1200 , and 1300°C . Inset: temperature variation of the magnetization measured at $H = 5000$ Oe.

deficient (2.95). This could be due to the error in the calculation (actual weight of the sample taken for measurement will be less due to the high carbon content in the sample as evidenced from XPS studies).

III. RESULTS AND DISCUSSION

A. Magnetization measurements

A magnetic transition below ~ 280 K is reported in the literature from studies on the magnetic properties of $\text{LaMn}_{0.5}\text{Ni}_{0.5}\text{O}_3$ (LMN) using high magnetic fields. Compared to the reports on the mixed-phase behavior observed for the related compound, $\text{LaMn}_{0.5}\text{Co}_{0.5}\text{O}_3$,^{12,31} there are no reports on the possible existence of two different magnetic phases for LMN, except for the observations by Sonobe and Asai in 1992,²⁰ who found, from powder XRD studies, the formation of a minor amount of a rhombohedral phase along with the orthorhombic phase of the compound. We have shown earlier that magnetic measurements using very low magnetic fields can detect the presence of different phases of ferromagnetic compounds, if they coexist in the samples.^{23,32,33} Therefore, zero-field-cooled magnetization (M_{ZFC}) measurements were made at a low magnetic field of 50 Oe, to look for the possible existence of different phases of $\text{LaMn}_{0.5}\text{Ni}_{0.5}\text{O}_3$, if any, in the HT and LT samples annealed at different temperatures.

1. HT samples

Figure 1 shows the ZFC magnetization curves of the $\text{LaMn}_{0.5}\text{Ni}_{0.5}\text{O}_3$ sample synthesized by the solid-state reaction method. Magnetization curves recorded after annealing the sample at 1100 , 1200 , and 1300°C are shown in the figure for comparison. Two well-defined magnetic transitions, at ~ 150 and ~ 280 K, are clearly visible in all the curves. There is no change in the onset of the magnetic tran-

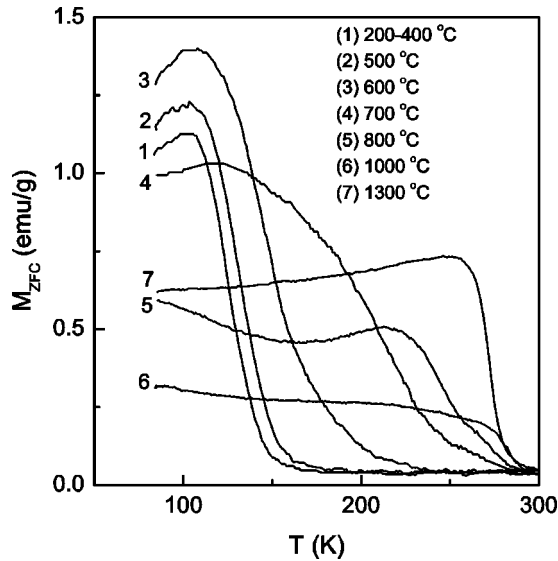


FIG. 2. ZFC magnetization curves ($H=50$ Oe) of the low-temperature synthesized $\text{LaMn}_{0.5}\text{Ni}_{0.5}\text{O}_3$ samples annealed in the temperature range 200–1300 °C.

sition temperatures or relative heights of the individual magnetic transitions even after heating at higher temperatures. From the two clear magnetic transitions at different temperatures, and when compared with the similar results obtained on $\text{LaMn}_{0.5}\text{Co}_{0.5}\text{O}_3$ samples prepared under identical conditions,²³ it appears that there are two possible ferromagnetic phases for $\text{LaMn}_{0.5}\text{Ni}_{0.5}\text{O}_3$. The inset in the figure shows the temperature variation of the magnetization of the sample heated at 1300 °C, measured at 5000 Oe. The high-field magnetization curve does not clearly show the two different magnetic transitions. The magnetic transition appears very broad, with the onset of the magnetic transition below 280 K. This high-field magnetization curve is similar to that reported by Sonobe and Asai for one of their samples,²⁰ measured at 18 kOe.

2. LT samples

Temperature variations of the zero-field-cooled magnetizations of $\text{LaMn}_{0.5}\text{Ni}_{0.5}\text{O}_3$ samples, synthesized by the low-temperature method, and annealed between 200 and 1300 °C are shown in Fig. 2. The magnetization curves of the samples annealed between 200 and 400 °C are identical, and the onset of a broad magnetic transition is observed below 160 K. Increasing the annealing temperature above 500 °C causes a broadening of the magnetic transition, with an increase in the value of the temperature at which the magnetization is increased from the base line. A sharp magnetic transition at 280 K is observed for the sample annealed at 1300 °C. By comparing the results for the LT samples with those obtained for the HT samples (see Fig. 3), it may be seen that the magnetic transition observed for the LT sample annealed at 400 °C is at the transition temperature of the first magnetic transition observed for the HT sample (~ 150 K). Similarly, the magnetic transition observed for the LT sample annealed at 1300 °C is at the transition temperature (~ 280 K) of the second magnetic transition observed for the HT sample. This

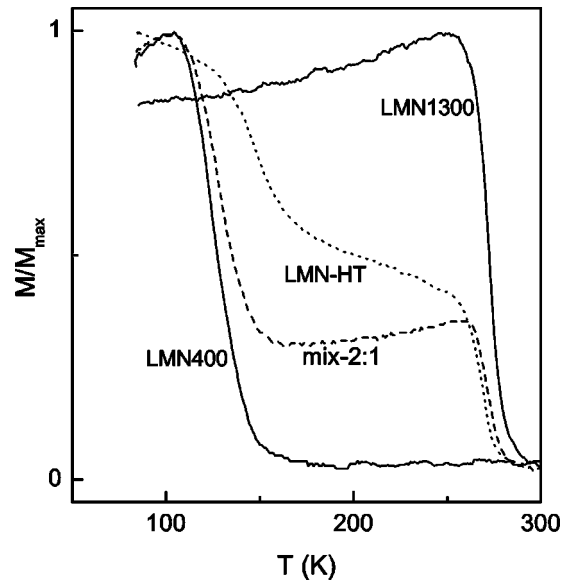


FIG. 3. Comparison of the ZFC magnetization curve ($H=50$ Oe) of the HT sample of $\text{LaMn}_{0.5}\text{Ni}_{0.5}\text{O}_3$ annealed at 1300 °C (LMN-HT) with the curves of the LT samples annealed at 400 °C (LMN400) and 1300 °C (LMN1300), and a 2:1 physical mixture of LMN400 and LMN1300 (mix-2:1).

indicates that the two different ferromagnetic phases of $\text{LaMn}_{0.5}\text{Ni}_{0.5}\text{O}_3$ can be obtained in single-phase forms by a low-temperature method of synthesis, and when heated below 500 °C and above 1200 °C. The ZFC magnetization curve of a physical mixture of the samples annealed at 400 and 1300 °C (a 2:1 ratio) is almost identical to that of the HT sample, suggesting that the HT sample contains almost a third of the phase showing a higher transition temperature. On the other hand, the broad magnetic transitions of the LT samples annealed between 600 and 1000 °C are indicative of a slow conversion of one phase in to the other.

From the studies on $\text{RMn}_{0.5}\text{Co}_{0.5}\text{O}_3$ with different rare earth ions ($R=\text{Pr, Nd, Sm}$), it was found that other rare-earth-containing compositions also show two different ferromagnetic phases when processed at different temperatures.³⁴ For both low- and high- T_c phases, the transition temperatures decrease with decreasing ionic size of the rare-earth ions.³⁵ To verify whether a similar two phase problem is encountered when La is replaced by other rare earth ions in $\text{LaMn}_{0.5}\text{Ni}_{0.5}\text{O}_3$ also, magnetic measurements were made on $\text{NdMn}_{0.5}\text{Ni}_{0.5}\text{O}_3$ (NMN) samples processed at different temperature. ZFC magnetization curves of NMN samples annealed at 400 and 1300 °C show magnetic transitions below 90 and 195 K, respectively, as shown in Fig. 4, indicating the possible formation of two different ferromagnetic phases of $\text{NdMn}_{0.5}\text{Ni}_{0.5}\text{O}_3$ as in the case of $\text{LaMn}_{0.5}\text{Ni}_{0.5}\text{O}_3$. The decrease in the magnetic transition temperatures, for both phases, when La^{3+} is replaced by Nd^{3+} with a lower ionic size, is due to the internal pressure effect as observed for $\text{RMn}_{0.5}\text{Co}_{0.5}\text{O}_3$.

B. Powder XRD studies

In the previous reports on $\text{LaMn}_{1-x}\text{Ni}_x\text{O}_3$,^{11,18,31} it was identified that all compositions up to $x=0.5$ in the series are

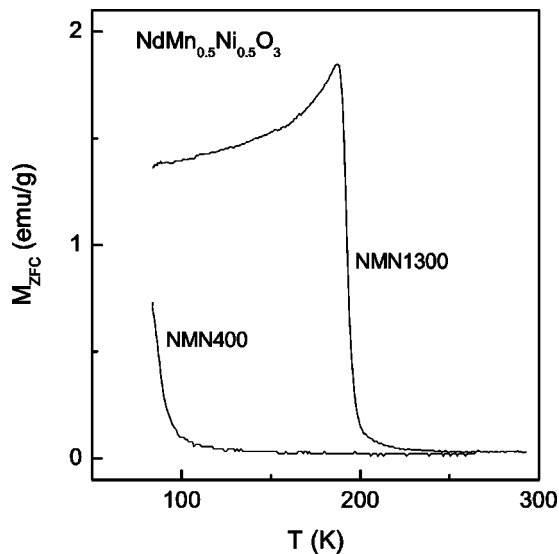


FIG. 4. ZFC magnetization curves ($H=50$ Oe) of the low-temperature synthesized $\text{NdMn}_{0.5}\text{Ni}_{0.5}\text{O}_3$ samples annealed at 400°C (NMN400) and 1300°C (NMN1300).

orthorhombic, and rhombohedral for $x > 0.5$. Wold *et al.* observed a slight monoclinic distortion for $x = 0.5$ and a monoclinic structure for $x > 0.5$.¹¹ However, considering the fact that the structure is orthorhombic for $x < 0.5$ including the end member LaMnO_3 and rhombohedral for $x > 0.5$ including the end member LaNiO_3 , it is possible that, for $x = 0.5$, two different phases with the above two structures may form simultaneously as observed in the case of $\text{LaMn}_{0.5}\text{Co}_{0.5}\text{O}_3$. As mentioned in Sec. I, Sonobe and Asai found the presence of nearly 10–25% of a rhombohedral phase in their $\text{LaMn}_{0.5}\text{Ni}_{0.5}\text{O}_3$ sample prepared by the ceramic method.²⁰

1. HT samples

The powder XRD pattern of the HT sample annealed at 1300°C (LMN-HT) is shown in Fig. 5. No impurity peaks are observed, indicating the formation of a perovskite phase. Wold *et al.*¹¹ and Troyanchuk *et al.*³¹ found that the crystal structure of $\text{LaMn}_{0.5}\text{Ni}_{0.5}\text{O}_3$, synthesized by the solid-state method, as orthorhombic. The powder XRD pattern of LMN-HT in Fig. 5 can be indexed on an orthorhombic structure with lattice parameters $a = 5.477 \text{ \AA}$, $b = 5.464 \text{ \AA}$, and $c = 7.670 \text{ \AA}$. These lattice parameters are almost comparable to those reported previously.^{11,31} However, magnetic measurements already indicated the presence of two ferromagnetic phases in this sample. Therefore, it is reasonable to assume that the observed pattern comprises of the contributions from these two different phases. The observed pattern could be fitted to $\sim 70\%$ of an orthorhombic phase ($a = 5.478 \text{ \AA}$, $b = 5.460 \text{ \AA}$, and $c = 7.672 \text{ \AA}$) and $\sim 30\%$ of a rhombohedral phase ($a = 5.426 \text{ \AA}$ and $\alpha = 60.9^\circ$). These values are comparable to that reported by Sonobe and Asai.²⁰ The ratio of the two phases found from powder XRD, in the HT sample, is in agreement with the magnetic measurements on a physical mixture of the two individual phases obtained by the low-temperature method of synthesis (see Fig. 3).

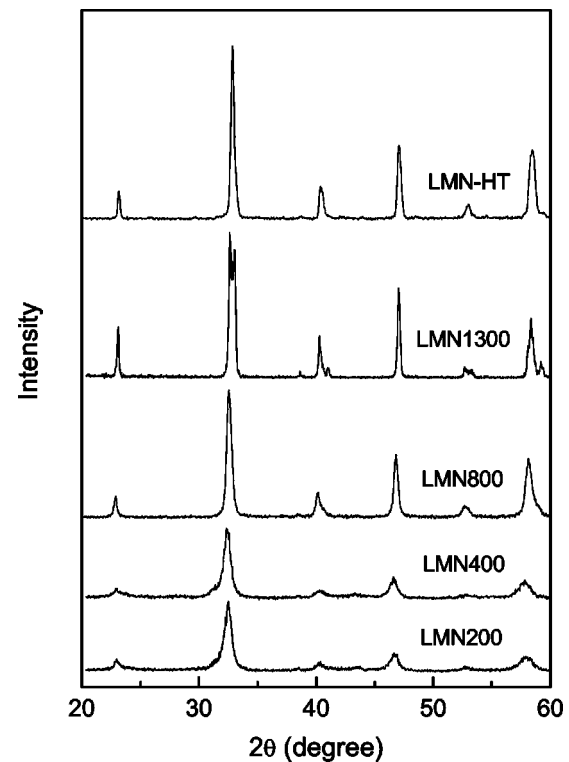


FIG. 5. Powder x-ray-diffraction patterns of the $\text{LaMn}_{0.5}\text{Ni}_{0.5}\text{O}_3$ samples synthesized by the ceramic method, annealed at 1300°C (LMN-HT), and the low-temperature method, annealed at 200°C (LMN200), 400°C (LMN400), 800°C (LMN800), and 1300°C (LMN1300).

2. LT samples

Powder XRD patterns of the LT samples of $\text{LaMn}_{0.5}\text{Ni}_{0.5}\text{O}_3$, annealed at 200°C (LMN200), 400°C (LMN400), 800°C (LMN800), and 1300°C (LMN1300) are compared in Fig. 5. All the reflections of LMN200 correspond to a perovskite phase, indicating the formation of $\text{LaMn}_{0.5}\text{Ni}_{0.5}\text{O}_3$ at 200°C . The XRD patterns of LMN200 and LMN400 are identical, and the reflections are very broad indicating the fine particle nature of the compound obtained at low temperatures. The average particle size is obtained as 13 nm from x-ray line broadening, calculated using the Scherrer formula,³⁶ $t = 0.9\lambda / \beta \cos \theta$; where t is the particle size, λ is the wave length of $\text{Cu } K\alpha$ radiation, β is the full width at half maximum of the diffraction peak corrected for instrumental broadening, and θ is the diffraction angle. The powder pattern of LMN200 could be indexed to an orthorhombic unit cell with lattice parameters $a = 5.50 \text{ \AA}$, $b = 5.65 \text{ \AA}$, and $c = 7.78 \text{ \AA}$. On the other hand, the XRD pattern of LMN1300 corresponds to the reflections from a rhombohedral lattice. The rhombohedral lattice parameters are obtained as $a = 5.428 \text{ \AA}$, and 60.9° . The powder pattern of LMN800, showing multiple magnetic transitions below $\sim 280 \text{ K}$, is almost identical to that of the sample prepared by the ceramic method showing two magnetic transitions. The pattern of LMN800 also is a mixture of an orthorhombic phase ($\sim 60\%$) and a rhombohedral phase ($\sim 40\%$).

In the case of perovskite type compounds, which are magnetic, it is known that the magnetic transition temperature depends on the structure of the compound. The highest Curie temperature is found for cubic phases, and the Curie temperature decreases when the structure is distorted to rhombohedral and then to orthorhombic.³⁷ This is because the strength of magnetic exchange interactions in the perovskites depends on interionic distances and bond angles. The B - O - B bond angle (in ABO_3) is decreased when the structure is distorted from cubic \rightarrow rhombohedral \rightarrow orthorhombic. This distortion modifies the magnetic transition temperature because T_c is determined by the strength of the exchange interactions due to orbital overlap between manganese and oxygen. The Curie temperature of the rhombohedral phase of $\text{LaMn}_{0.5}\text{Co}_{0.5}\text{O}_3$ was found to be larger than that of the orthorhombic phase, and similar results are observed here for $\text{LaMn}_{0.5}\text{Ni}_{0.5}\text{O}_3$ also, which is in accordance with the observations of the structural dependence of T_c .

From zero-field-cooled magnetization measurements using low magnetic fields and powder XRD measurements, it is now obvious that $\text{LaMn}_{0.5}\text{Ni}_{0.5}\text{O}_3$ can form in two different crystallographic forms with different magnetic transition temperatures. Having found that $\text{LaMn}_{0.5}\text{Ni}_{0.5}\text{O}_3$, synthesized by the high-temperature ceramic method, is multiphase due to the presence of two different phases of the compound, and that single phase compounds are obtained from samples synthesized by the low-temperature method and annealed at 400 and 1300 °C, we have studied these two samples in detail to understand the difference between the two different phases of the compound. High-temperature paramagnetic susceptibility and core-level XPS studies were performed on these two samples (LMN400 and LMN1300) to obtain information on the spin states of Mn and Ni in $\text{LaMn}_{0.5}\text{Ni}_{0.5}\text{O}_3$.

C. Magnetic susceptibility studies

The temperature dependence of the inverse of the paramagnetic susceptibility (>300 K) of LMN400 and LMN1300 is shown in Fig. 6. The susceptibility of LMN400 is measured up to 573 K (300 °C) only, which is well within the stability temperature of this phase. The susceptibility of LMN1300 is measured up to 723 K (450 °C), as this phase is stable in this temperature range. A Curie-Weiss behavior $\chi = C/(T - \Theta)$, is observed for both samples. The effective paramagnetic moment $\mu_{eff} = 2.828\sqrt{C}$, where C is the Curie constant, is obtained from a least-squares fit to the data in the linear region at high temperatures. Almost identical slopes with different intercepts on the temperature axis are obtained for both samples. μ_{eff} is obtained as $3.54 \mu_B$ and $3.57 \mu_B$ for the two samples LMN400 and LMN1300, respectively, and the corresponding paramagnetic Curie temperatures (Θ) are obtained as 192 and 313 K.

The spin-only values of the moment, μ_{so} , for various possible combinations of different spin states of Mn and Ni in $\text{LaMn}_{0.5}\text{Ni}_{0.5}\text{O}_3$ are compared in Table I. The experimental μ_{eff} values ($3.54 \mu_B$ and $3.57 \mu_B$) are comparable to the spin-only moments calculated for high-spin Mn^{3+} and low-spin Ni^{3+} as well as for Mn^{4+} and Ni^{2+} . Therefore, it is

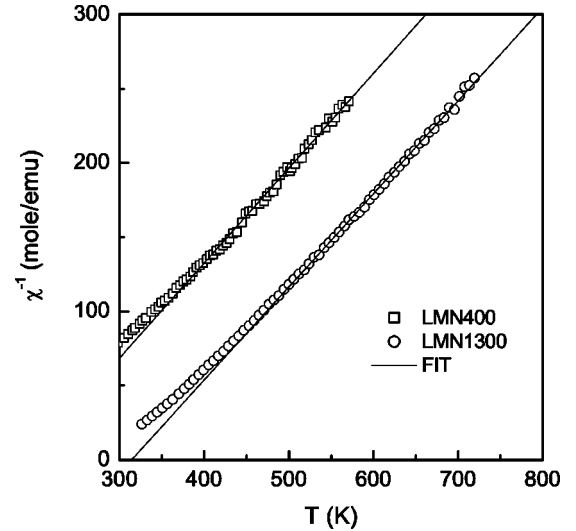


FIG. 6. Temperature variation of the inverse of the paramagnetic susceptibility of LMN400 and LMN1300.

possible that the spin states of Mn and Ni in LMN400 and LMN1300 are either identical or have the above two different combinations. The different values of the paramagnetic Curie temperatures obtained from a Curie-Weiss fit to the susceptibility data indicate a difference in the strength of the magnetic exchange interactions and, therefore, a possible difference in the spin states of Mn and Ni in LMN400 and LMN1300. In the case of $\text{LaMn}_{0.5}\text{Co}_{0.5}\text{O}_3$, a higher Curie temperature was found for its rhombohedral phase containing Mn^{3+} ions and low-spin Co^{3+} ions. The fact that a higher Curie temperature is obtained for LMN1300, which is rhombohedral, implies that the possible spin states in LMN1300 are Mn^{3+} and low-spin Ni^{3+} ($\mu_{eff} = 3.57 \mu_B$ and $\mu_{so} = 3.67 \mu_B$). Assuming that LMN400 contains Mn^{4+} and Ni^{2+} , as observed in the case of $\text{LaMn}_{0.5}\text{Co}_{0.5}\text{O}_3$, then the higher value of μ_{eff} of LMN400 when compared to μ_{so} calculated for Mn^{4+} and Ni^{2+} can be accounted for, considering the contribution from the spin-orbit coupling of Ni^{2+} . A slightly larger value of μ_{eff} can be expected for Ni^{2+} due to the contribution from spin-orbit coupling, as generally observed.³⁸ Usually the average magnetic moment calculated for the ${}^3A_{2g}$ ground term of Ni^{2+} , incorporating the contribution from spin-orbit coupling, using $\bar{\mu}_e = \mu_{so}(1 - 4\lambda/10Dq)$, where λ is the spin-orbit coupling coefficient,

TABLE I. Comparison of the spin-only moments (μ_{so}) for various spin states of Mn and Ni in $\text{LaMn}_{0.5}\text{Ni}_{0.5}\text{O}_3$.

Spin states	$\mu_{so}(\mu_B)^1$
Mn^{3+} ($S=2$), Ni^{3+} ($S=3/2$)	4.41
Mn^{3+} ($S=2$), Ni^{3+} ($S=1/2$)	3.67
Mn^{4+} ($S=3/2$), Ni^{2+} ($S=1$)	3.39
Mn^{2+} ($S=5/2$), Ni^{4+} ($S=2$)	5.43
Mn^{2+} ($S=5/2$), Ni^{4+} ($S=1$)	4.64
Mn^{2+} ($S=5/2$), Ni^{4+} ($S=0$)	4.18

$${}^1\mu_{so} = [0.5\mu_{Mn}^2 + 0.5\mu_{Ni}^2]^{1/2}, \mu = [4S(S+1)]^{1/2}$$

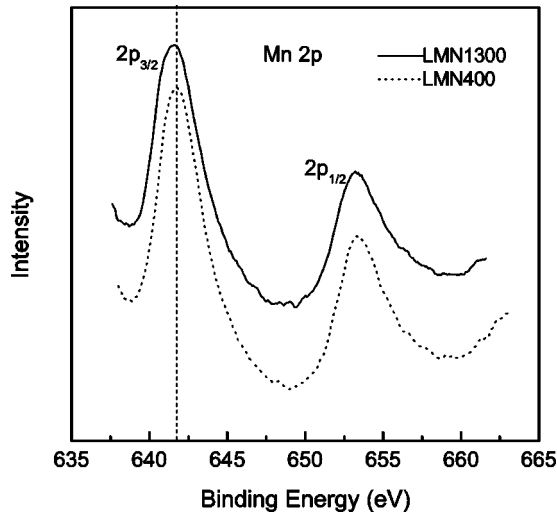


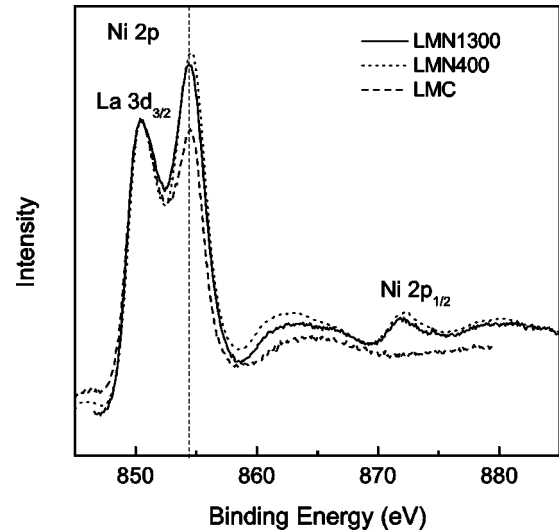
FIG. 7. Mn 2p XPS of LMN400 and LMN1300.

Dq is the crystal-field splitting parameter, and $\mu_{so} = 2.83 \mu_B$, is $\sim 3.25 \mu_B$. Using this value of $\bar{\mu}_e$, the calculated moment for Mn^{4+} and Ni^{2+} in $LaMn_{0.5}Ni_{0.5}O_3$ would be $3.58 \mu_B$ which is comparable to the experimental value of $3.54 \mu_B$ for LMN400. Therefore, if the contribution from the spin-orbit coupling of Ni^{2+} is taken into account, it may be considered that the combination of the spin states Mn^{4+} and Ni^{2+} is possible in LMN400.

D. XPS studies

Core-level x-ray photoelectron spectroscopic studies were performed on LMN400 and LMN1300 to confirm the results obtained from high-temperature magnetic susceptibility studies. Core-level XPS's of the transition-metal ions are known to be sensitive to their spin-states and 3d-electron contents. There is a general trend that the core-level binding energy increases with the increasing oxidation state of a given ion, provided that the ions are located in similar coordination environments in different compounds. However, this rule breaks down when the number of unpaired electrons changes due to a change in the spin state of a given ion. It was reported earlier that under identical octahedral coordination environments, the $2p_{3/2}$ binding energy (BE) of low-spin Co^{3+} is lower than that of Co^{2+} .^{39,40} Similarly, it was found that the Ni $2p_{3/2}$ BE of Ni_2O_3 containing low-spin Ni^{3+} is lower than that of NiO containing Ni^{2+} .^{41,42}

The $2p$ core-level XPS's of Mn in LMN400 and LMN1300 are compared in Fig. 7. The binding energy of Mn $2p_{3/2}$ is obtained as 641.8 eV for LMN400 and as 641.5 eV for LMN1300. Generally the $2p_{3/2}$ BE is found to be lower for Mn^{3+} than for Mn^{4+} , when the ions are situated in identical environments (as in $LaMn^{3+}O_3$ and $CaMn^{4+}O_3$) by 0.3–0.4 eV. The difference between the BE's of Mn $2p_{3/2}$ obtained for the two samples of $LaMn_{0.5}Ni_{0.5}O_3$ is identical to that found for the two different phases of $LaMn_{0.5}Co_{0.5}O_3$ having different spin states of Mn, Mn^{3+} for the high- T_c phase and Mn^{4+} for the low- T_c phase.²⁴ In the case of $LaMn_{0.5}Co_{0.5}O_3$ also, a lower BE is obtained for the sample

FIG. 8. Ni 2p XPS of LMN400 and LMN1300, along with the La $3d_{3/2}$ XPS of $LaMn_{0.5}Co_{0.5}O_3$ (LMC).

with a higher T_c , indicating that the spin state of Mn is Mn^{3+} in LMN1300 and Mn^{4+} in LMN400.

Figure 8 shows the $2p$ core-level XPS of Ni in LMN400 and LMN1300. Unfortunately, the binding energy of the satellite peak of La $3d_{3/2}$ is almost identical to the BE of $2p_{3/2}$ of Ni in oxides, and therefore these peaks overlap for compounds containing both La and Ni. The main and satellite peaks of La $3d_{3/2}$ in La_2O_3 and other perovskite-type oxides are observed with an intensity ratio of approximately 1:1,⁴³ as shown in Fig. 8 for $LaMn_{0.5}Co_{0.5}O_3$. Therefore, the larger intensity of the peak in the BE region of the satellite peak of La $3d_{3/2}$ may be considered as the contribution of Ni $2p_{3/2}$ for both LMN400 and LMN1300. Since the La^{3+} ion is situated in the same environment in both LMN400 and LMN1300, and the BE of the La $3d_{3/2}$ main peak is identical for both samples (the intensities of this peak is normalized for all samples in the figure), it may be assumed that the small difference in the BE of the peak in the region of the La $3d_{3/2}$ satellite peak is due to the difference in the BE of Ni $2p_{3/2}$ in the two samples. This comparison gives a Ni $2p_{3/2}$ BE of 854.6 eV for LMN400 and 854.3 eV for LMN1300. A similar difference in the BE is also observed for the Ni $2p_{1/2}$ peaks for the two compounds. The differences in the binding energies of Ni $2p_{3/2}$ and $2p_{1/2}$ are $\Delta E = 17.8$ eV for LMN400 and $\Delta E = 17.6$ eV for LMN1300, respectively. The lower value of ΔE for LMN1300 by 0.2 eV may be taken as evidence that there is one less unpaired electron in Ni in this sample. This fact, when combined with the lower BE of the Ni $2p_{3/2}$ peak, then corresponds to the spin state of Ni as low-spin Ni^{3+} ($S = 1/2$) in LMN1300 and as Ni^{2+} ($S = 1$) in LMN400. These spin states of Ni in the two samples are similar to that observed for Co in the nanocrystalline and high-temperature heated samples of $LaMn_{0.5}Co_{0.5}O_3$.²⁵ A lower BE is expected for low-spin Ni^{3+} when compared to the higher BE of Ni^{2+} , due to the lower number of unpaired electrons in the former. Moreover, these spin states of Ni in the two samples are in accordance with the spin states of Mn, which will take care of charge neutrality and oxygen stoichiometry.

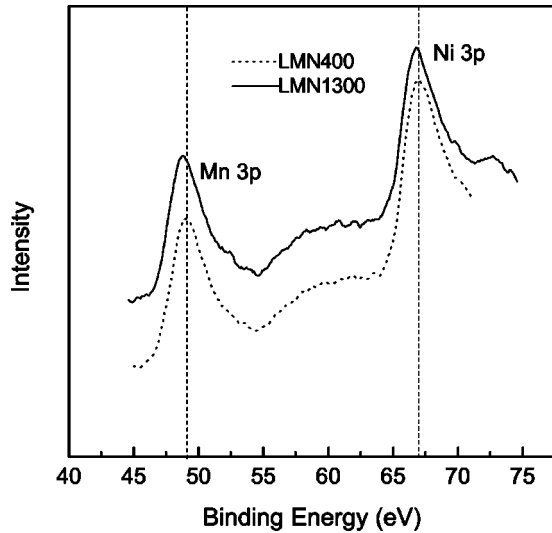


FIG. 9. Mn and Ni 3p XPS of LMN400 and LMN1300.

A comparison of Mn and Ni 3p XPS's, shown in Fig. 9, of LMN400 and LMN1300, also shows the same trend in the binding energies. Mn 3p XPS peaks are observed at 49.1 and 48.8 eV, and Ni 3p peaks are observed at 66.9 and 66.7 eV, respectively, for LMN400 and LMN1300. This gives further evidence of the different spin states of Mn and Ni in the two samples, as concluded from the analysis of the 2p XPS of Mn and Ni.

The overlapping of the Ni 2p_{3/2} XPS peaks with that of La 3d_{3/2} satellite peak for compounds containing both La and Ni can be taken care of by selecting another rare-earth ion, whose XPS peaks will not interfere with that of Ni 2p_{3/2}, in the same composition. To compare the differences in the Ni 2p_{3/2} XPS binding energies of the compounds heated at 400 and 1300 °C, and to further confirm the observations made on LaMn_{0.5}Ni_{0.5}O₃, core-level XPS studies were made on NdMn_{0.5}Ni_{0.5}O₃ (NMN) samples processed

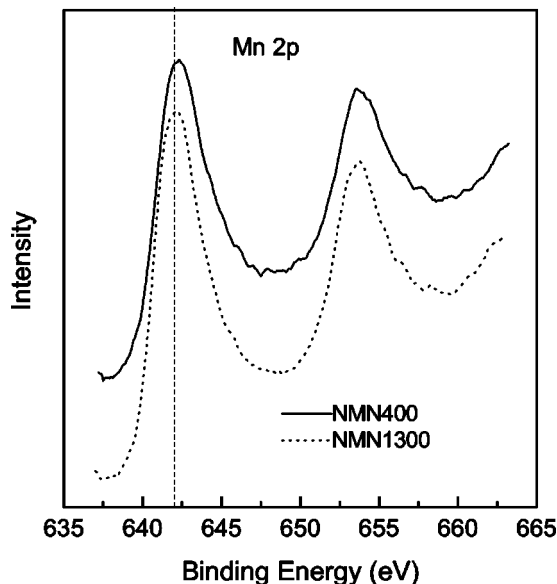


FIG. 10. Mn 2p XPS of NMN400 and NMN1300.

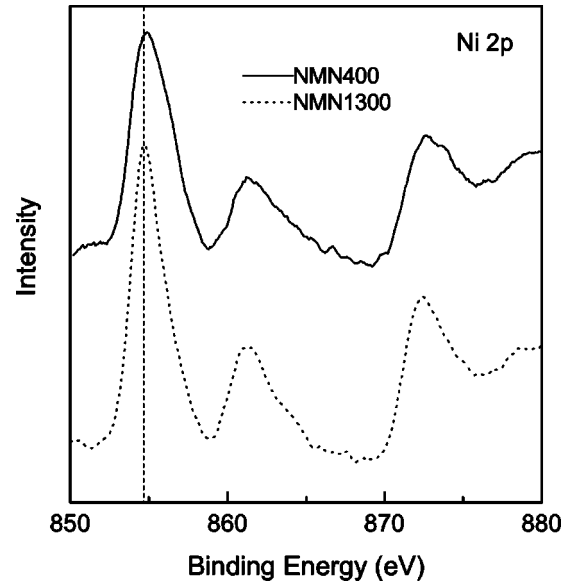


FIG. 11. Ni 2p XPS of NMN400 and NMN1300.

under identical conditions. Mn and Ni 2p XPS's of the two samples of NMN, heated at 400 and 1300 °C (NMN400 and NMN1300), and showing magnetic transitions at different temperatures, are shown in Figs. 10 and 11, respectively. The Mn 2p_{3/2} and Ni 2p_{3/2} XPS binding energies of Mn and Ni in LMN and NMN are compared in Table II. There is a small shift in the BE's of the XPS peaks to higher values by ~0.5 eV when La is replaced by Nd. Similar effects have been generally observed in the XPS studies on different rare-earth compounds.⁴⁴⁻⁴⁶

As expected, there is a difference in the binding energies of the Mn as well as Ni 2p XPS peaks of NMN400 and NMN1300. As observed for the corresponding LMN samples, the Ni 2p_{3/2} binding energy is lower by 0.2 eV for NMN1300, showing a magnetic transition at a higher temperature when compared to NMN400, confirming that the spin state of Ni is Ni²⁺ in the sample showing a lower magnetic transition temperature and low-spin Ni³⁺ for the high-T_c phase with rhombohedral symmetry. A similar difference in the Mn 2p_{3/2} BE energy is also observed for the two NMN samples, indicating the presence of Mn⁴⁺ and Mn³⁺ in the samples heated at 400 and 1300 °C, respectively.

E. Charge disproportionation and magnetic exchange interactions in LaMn_{0.5}Ni_{0.5}O₃

The results from high-temperature paramagnetic susceptibility and core-level XPS studies confirm that the spin states of Mn and Ni are different in the two ferromagnetic phases of LaMn_{0.5}Ni_{0.5}O₃ obtained at different processing temperatures. The different spin states of Mn and Ni, Mn⁴⁺ and Ni²⁺ in LMN400 (low-T_c phase) and Mn³⁺ and low-spin Ni³⁺ in LMN1300 (high-T_c phase), explain the different magnetic transition temperatures of these two samples of LaMn_{0.5}Ni_{0.5}O₃, and point to the existence of two possible phases of the compound. The different spin states of Mn and Ni in LMN400 and LMN1300 show the charge disproportionation

TABLE II. Comparison of the Mn $2p_{3/2}$ and Ni $2p_{3/2}$ XPS binding energies of Mn and Ni in the two different ferromagnetic phases of $\text{LaMn}_{0.5}\text{Ni}_{0.5}\text{O}_3$ (LMN) and $\text{NdMn}_{0.5}\text{Ni}_{0.5}\text{O}_3$ (NMN).

Compound	Sample	T_c (K)	Mn $2p_{3/2}$ (eV)	Ni $2p_{3/2}$ (eV)
$\text{LaMn}_{0.5}\text{Ni}_{0.5}\text{O}_3$	LMN400	150	641.8	854.6
	LMN1300	280	641.5	854.3
$\text{NdMn}_{0.5}\text{Ni}_{0.5}\text{O}_3$	NMN400	90	642.4	854.9
	NMN1300	195	642.1	854.7

tionation $\text{Mn}^{4+} + \text{Ni}^{2+} \rightarrow \text{Mn}^{3+} + \text{Ni}^{3+}$ when the low-temperature synthesized samples are heated to higher temperatures. The broader or multiple magnetic transitions observed for samples heated in the temperature range 400–1200 °C are then due to the mixed valence states of Mn and Ni (due to slow and partial charge disproportionations when sufficient thermal energy is not available) and, therefore, due to the different types of superexchange interactions in these samples. As observed for $\text{LaMn}_{0.5}\text{Co}_{0.5}\text{O}_3$, a higher Curie temperature is observed for a phase containing Mn^{3+} , suggesting that $\text{Mn}^{3+}\text{-O-Mn}^{3+}$ superexchange interactions are stronger than that of the $\text{Mn}^{4+}\text{-O-M}^{2+}$ ($M = \text{Co, Ni}$) interactions.

The Curie temperature of $\text{LaMn}_{0.5}^{3+}\text{Ni}_{0.5}^{3+}\text{O}_3$ (280 K) is larger than that of the corresponding Co-containing composition $\text{LaMn}_{0.5}^{3+}\text{Co}_{0.5}^{3+}\text{O}_3$ (230 K). This is possibly due to the major contribution from $\text{Mn}^{3+}\text{-O-Ni}^{3+}$ or $\text{Ni}^{3+}\text{-O-Ni}^{3+}$ superexchange interactions, as discussed in detail by Goodenough and co-workers.^{11,12} It may be noted that the low-spin Ni^{3+} , with an electronic configuration $t_{2g}^6 e_g^1$, contains one unpaired electron ($S = 1/2$), when compared to the diamagnetic ($S = 0$), low-spin, Co^{3+} ion ($t_{2g}^6 e_g^0$). Therefore, the magnetic exchange interaction of the type $\text{Mn}^{3+}\text{-O-M}^{3+}\text{-O-Mn}^{3+}$ would be stronger when $M = \text{Ni}$. To understand the role of Ni in the magnetic exchange interactions in $\text{LaMn}_{0.5}\text{Ni}_{0.5}\text{O}_3$, part of Mn^{3+} or Ni^{3+} was substituted by the non-magnetic ion, Al^{3+} . $\text{LaMn}_{0.5}\text{Ni}_{0.4}\text{Al}_{0.1}\text{O}_3$ and $\text{LaMn}_{0.4}\text{Al}_{0.1}\text{Ni}_{0.5}\text{O}_3$ were prepared by the low-temperature method and heated at 1300 °C. The temperature dependence of the magnetization of $\text{LaMn}_{0.5}\text{Ni}_{0.5}\text{O}_3$ (LMN), $\text{LaMn}_{0.5}\text{Ni}_{0.4}\text{Al}_{0.1}\text{O}_3$ (LMNA), and $\text{LaMn}_{0.4}\text{Al}_{0.1}\text{Ni}_{0.5}\text{O}_3$ (LMAN), measured using $H = 5000$ Oe, is compared in Fig. 12. Measurements were made using a high magnetic field to compare the effect of substitution of Al on the magnitude of magnetization as well as on the Curie temperature. There is a drastic reduction in the magnetization when both Mn^{3+} and Ni^{3+} are partially replaced by Al^{3+} . The magnetization at the lowest temperature is reduced to 36% when Ni is substituted by Al and to 19% when Mn is substituted by Al. Similarly, the Curie temperature (the temperature at which a sharp transition is observed in M_{ZFC} measurements using $H = 50$ Oe) is reduced from 280 to 250 K when Ni is substituted and to 210 K when Mn is substituted. When a similar substitution was made on the corresponding Co composition $\text{LaMn}_{0.5}\text{Co}_{0.5}\text{O}_3$,²⁴ it was found that magnetization and T_c was not much affected on replacing Co by Al. The reduction

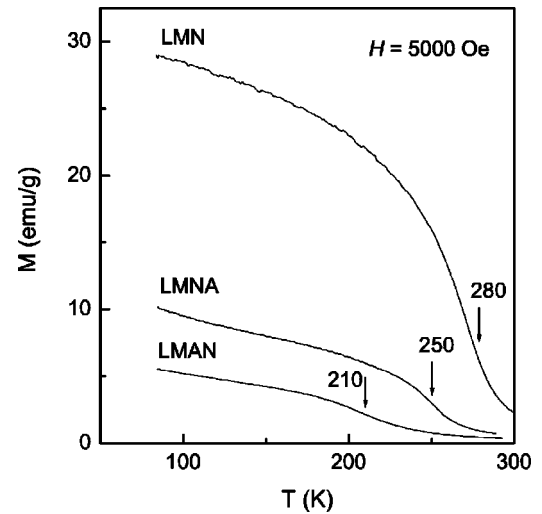


FIG. 12. Temperature variation of the magnetization of $\text{LaMn}_{0.5}\text{Ni}_{0.5}\text{O}_3$ (LMN), $\text{LaMn}_{0.5}\text{Ni}_{0.4}\text{Al}_{0.1}\text{O}_3$ (LMNA), and $\text{LaMn}_{0.4}\text{Al}_{0.1}\text{Ni}_{0.5}\text{O}_3$ (LMAN); $H = 5000$ Oe.

in both magnetization and Curie temperature when Ni is replaced by Al indicates the direct role of Ni^{3+} in determining the higher T_c of $\text{LaMn}_{0.5}\text{Ni}_{0.5}\text{O}_3$ when compared to the T_c of $\text{LaMn}_{0.5}\text{Co}_{0.5}\text{O}_3$.

Though there is a similarity in the properties and spin states of the transition-metal ions in the two compounds $\text{LaMn}_{0.5}\text{Ni}_{0.5}\text{O}_3$ and $\text{LaMn}_{0.5}\text{Co}_{0.5}\text{O}_3$, there is a major difference during the evolution of the phases having a higher Curie temperature. In the case of $\text{LaMn}_{0.5}\text{Co}_{0.5}\text{O}_3$, the sample annealed at lower temperatures (< 500 °C), containing Mn^{4+} and Co^{2+} , is converted to a phase with a higher T_c after annealing at 700 °C which contains Mn^{3+} and Co^{3+} which is again converted back at higher temperatures to a phase containing Mn^{4+} and Co^{2+} and having the same T_c as that obtained after heating at 400 °C.²⁵ That is, there is an unusual double charge disproportionation $\text{Mn}^{4+} + \text{Co}^{2+} \rightarrow \text{Mn}^{3+} + \text{Co}^{3+} \rightarrow \text{Mn}^{4+} + \text{Co}^{2+}$, indicating the stability of the low- T_c phase of the compound having an orthorhombic structure. On the other hand, in the case of $\text{LaMn}_{0.5}\text{Ni}_{0.5}\text{O}_3$, the sample formed initially at 200 °C with a lower T_c (having Mn^{4+} and Ni^{2+}) is slowly converted to a phase with a higher T_c (having Mn^{3+} and Ni^{3+}), and it did so only after heating at higher temperatures (1300 °C). There is no formation of a different phase of this compound after heating at intermediate temperatures, and the phase containing Mn^{3+} and Ni^{3+} is not reverted back to a low- T_c phase after heating at high temperatures. That is, there is only one stage of charge disproportionation as $\text{Mn}^{4+} + \text{Ni}^{2+} \rightarrow \text{Mn}^{3+} + \text{Ni}^{3+}$ in the case of $\text{LaMn}_{0.5}\text{Ni}_{0.5}\text{O}_3$, as against the double charge disproportionation observed in the case of $\text{LaMn}_{0.5}\text{Co}_{0.5}\text{O}_3$.

The phenomenal difference in the evolution of the different phases when $M = \text{Co}$ and Ni in La_2MnMO_6 may be due to the fact that the rhombohedral phase of $\text{LaMn}_{0.5}\text{Ni}_{0.5}\text{O}_3$ is energetically more stable than the orthorhombic phase, as against the more stable orthorhombic phase of $\text{LaMn}_{0.5}\text{Co}_{0.5}\text{O}_3$ compared to its rhombohedral form, as evidenced from energy density calculations by Yang *et al.*⁴⁷ From band structure calculations of the electronic and mag-

netic properties of rhombohedral $\text{LaMn}_{0.5}\text{Ni}_{0.5}\text{O}_3$, Yang *et al.*,⁴⁸ found that there is no difference between the charge occupation of Ni ions in the compound and LaNiO_3 (low-spin Ni^{3+}). Similarly, the charge distribution of Mn ions in the compound was found to be the same as that in LaMnO_3 (Mn^{3+}). The present results are in agreement with the band-structure calculations. One of the interesting aspects of the high- T_c phase of $\text{LaMn}_{0.5}\text{Ni}_{0.5}\text{O}_3$ is that both the B-site ions, Mn^{3+} and low-spin Ni^{3+} , are Jahn-Teller ions (one unpaired electron in the e_g orbital in both cases). This may be responsible for the additional stability of the rhombohedral phase of $\text{LaMn}_{0.5}\text{Ni}_{0.5}\text{O}_3$ containing Mn^{3+} and Ni^{3+} . It may be possible that the rhombohedral structure is favored because of the net effect of the Jahn-Teller distortions of Mn^{3+} and low-spin Ni^{3+} . Only Mn^{3+} ions are JT ions in $\text{LaMn}_{0.5}\text{Co}_{0.5}\text{O}_3$, and the rhombohedral structure is less stable due to this distortion, giving rise to the charge disproportionation $\text{Mn}^{3+} + \text{Co}^{3+} \rightarrow \text{Mn}^{4+} + \text{Co}^{2+}$ having a more stable orthorhombic structure.

IV. CONCLUSIONS

The properties of $\text{LaMn}_{0.5}\text{Ni}_{0.5}\text{O}_3$, synthesized by ceramic and low-temperature methods of synthesis, have been studied in detail to understand the origin of ferromagnetism in this compound. Two magnetic transitions are observed in the sample synthesized by the high-temperature ceramic method, due to the presence of two different phases of the compound. The two phases are obtained in single-phase forms by a low-temperature method of synthesis. One phase showing a magnetic transition below 160 K is found to be stable only below 500 °C, and is converted to the second phase having a higher magnetic transition temperature (280 K) after heating at higher temperatures, so that both phases coexist in samples processed in the temperature range 500–1300 °C. This explains why two magnetic transitions are observed in the

samples synthesized by the usual high-temperature ceramic method. The crystal structures of the two phases are also found to be different: orthorhombic for the low- T_c phase and rhombohedral for the high- T_c phase. High-temperature magnetic susceptibility studies on samples annealed at 400 and 1300 °C gave comparable values for the effective magnetic moment, with a large difference in the paramagnetic Curie temperature, indicating the different strengths of magnetic exchange interactions in the two samples. The effective paramagnetic moment values obtained for the two phases are comparable to the spin-only moments calculated for a combination of different spin states of Mn and Ni: Mn^{3+} and low-spin Ni^{3+} for one phase and Mn^{4+} and Ni^{2+} for the other phase. A comparison of the results obtained on the similar compound $\text{LaMn}_{0.5}\text{Co}_{0.5}\text{O}_3$ and core-level x-ray photoelectron spectroscopic studies give conclusive evidence for different spin states of Mn and Ni in the two phases: Mn^{4+} and Ni^{2+} in the nanocrystalline material showing a magnetic transition at a lower temperature, and Mn^{3+} and low-spin Ni^{3+} in the high- T_c phase. These results indicate a possible charge disproportionation, $\text{Mn}^{4+} + \text{Ni}^{2+} \rightarrow \text{Mn}^{3+} + \text{Ni}^{3+}$, when the low-temperature synthesized sample is heated in the temperature range 400–1300 °C. The results also indicate that the rhombohedral phase of the compound containing Mn^{3+} and Ni^{3+} is more stable. This is contrary to the results obtained for $\text{LaMn}_{0.5}\text{Co}_{0.5}\text{O}_3$, the orthorhombic phase having Mn^{4+} and Co^{2+} is found to be more stable. This difference in the stability of the different phases when $M = \text{Co}$ or Ni in $\text{LaMn}_{0.5}M_{0.5}\text{O}_3$ may be attributed to the presence of the two different Jahn-Teller ions, Mn^{3+} and low-spin Ni^{3+} in the case of $\text{LaMn}_{0.5}\text{Ni}_{0.5}\text{O}_3$.

ACKNOWLEDGMENTS

One of the authors (V.L.J.J.) is grateful to UGC, India, for financial support.

*Electronic address: joy@dalton.ncl.res.in; URL: <http://www.ncl-india.org>

¹K.-I. Kobayashi, T. Kimura, H. Sawada, K. Terakura, and Y. Tokura, *Nature (London)* **395**, 677 (1998).

²Y. Tomioka, T. Okuda, Y. Okimoto, R. Kumai, K.-I. Kobayashi, and Y. Tokura, *Phys. Rev. B* **61**, 422 (2000).

³J.B. Goodenough and R.I. Dass, *Int. J. Inorg. Mater.* **2**, 3 (2000).

⁴S. Nakayama, T. Nakagawa, and S. Nomura, *J. Phys. Soc. Jpn.* **24**, 219 (1968).

⁵J.M. Greneche, M. Venkatesan, R. Suryanarayanan, and J.M.D. Coey, *Phys. Rev. B* **63**, 174403 (2001).

⁶A.W. Sleight and J.F. Weiher, *J. Phys. Chem. Solids* **33**, 679 (1972).

⁷K. Ueda, Y. Muraoka, H. Tabata, and T. Kawai, *Appl. Phys. Lett.* **78**, 512 (2001).

⁸H. Falcon, A.E. Goeta, G. Punte, and R.E. Carbonio, *J. Solid State Chem.* **133**, 379 (1997).

⁹K. Ramesha, V. Thangadurai, D. Sutar, S.V. Subramanyam, G.N. Subbanna, and J. Gopalakrishnan, *Mater. Res. Bull.* **35**, 559 (2000).

¹⁰M. Wakeshima, Y. Izumiyama, Y. Doi, and Y. Hinatsu, *Solid State*

Commun. **120**, 273 (2001).

¹¹A. Wold, R.J. Arnott, and J.B. Goodenough, *J. Appl. Phys.* **29**, 387 (1958).

¹²J.B. Goodenough, A. Wold, R.J. Arnott, and N. Menyuk, *Phys. Rev.* **124**, 373 (1961).

¹³G. Blasse, *J. Phys. Chem. Solids* **26**, 1969 (1965).

¹⁴G.H. Jonker, *J. Appl. Phys.* **37**, 1424 (1966).

¹⁵H. Fujiki and S. Nomura, *J. Phys. Soc. Jpn.* **23**, 648 (1967).

¹⁶S.K. Dey, *Philos. Mag.* **16**, 1097 (1967).

¹⁷J.B. Goodenough and J.M. Longo, in *Magnetic Oxides and Related Compounds*, edited by K.-H. Hellwege, A.M. Hellwege, Landolt-Bornstein, New Series, Group III, Vol. 4, Pt. a (Springer, Berlin, 1970) p. 126.

¹⁸N.Y. Vasanthacharya, P. Ganguly, J.B. Goodenough, and C.N.R. Rao, *J. Phys. C* **17**, 2745 (1984).

¹⁹K. Asai, H. Sekizawa, and S. Iida, *J. Phys. Soc. Jpn.* **47**, 1054 (1979).

²⁰M. Sonobe and K. Asai, *J. Phys. Soc. Jpn.* **61**, 4193 (1992).

²¹N. Nishimori, K. Asai, and M. Mizoguchi, *J. Phys. Soc. Jpn.* **64**, 1326 (1995).

²²P.A. Joy, Y.B. Kholam, S.N. Patole, and S.K. Date, *Mater. Lett.* **46**, 261 (2000).

- ²³P.A. Joy, Y.B. Kholam, and S.K. Date, Phys. Rev. B **62**, 8608 (2000).
- ²⁴V.L. Joseph Joly, P.A. Joy, S.K. Date, and C.S. Gopinath, J. Phys.: Condens. Matter **13**, 649 (2001).
- ²⁵V.L. Joseph Joly, Y.B. Kholam, P.A. Joy, C.S. Gopinath, and S.K. Date, J. Phys.: Condens. Matter **13**, 11001 (2001).
- ²⁶E.O. Wollan and W.C. Koehler, Phys. Rev. **100**, 545 (1955).
- ²⁷J.-S. Zhou and J.B. Goodenough, Phys. Rev. B **60**, R15 002 (1999).
- ²⁸J. Kanamori, J. Appl. Phys. **31**, 14S (1960).
- ²⁹L.A. Chick, L.R. Pederson, G.D. Moupin, D.L. Bates, L.E. Thomas, and G.J. Exarhos, Mater. Lett. **10**, 6 (1990).
- ³⁰M.S.G. Baythoun and F.R. Sale, J. Mater. Sci. **17**, 2757 (1982).
- ³¹I.O. Troyanchuk, N.V. Samsonenko, E.F. Shapovalova, H. Szymczak, and A. Nabialek, Mater. Res. Bull. **32**, 67 (1997).
- ³²P.A. Joy, S.K. Date, and P.S. Anil Kumar, Phys. Rev. B **56**, 2324 (1997).
- ³³P.A. Joy, S.K. Date, and P.S. Anil Kumar, J. Appl. Phys. **83**, 6536 (1998).
- ³⁴V.L. Joseph Joly, P.A. Joy, and S.K. Date, Mater. Lett. **51**, 172 (2001).
- ³⁵V.L. Joseph Joly, P.A. Joy, and S.K. Date, Solid State Commun. **121**, 219 (2002).
- ³⁶B.D. Cullity, *Elements of X-Ray Diffraction* (Addison-Wesley, Reading, MA, 1956), p. 99.
- ³⁷J.M.D. Coey, M. Viret, and S. von Molnar, Adv. Phys. **48**, 167 (1999).
- ³⁸E.A. Boudreaux and L.N. Mulay, *Theory and Applications of Molecular Paramagnetism* (Wiley, New York, 1976), p. 54.
- ³⁹D. Briggs and V.A. Gibson, Chem. Phys. Lett. **25**, 493 (1974).
- ⁴⁰D.C. Frost, C.A. McDowell, and I.S. Woolsey, Chem. Phys. Lett. **17**, 320 (1972).
- ⁴¹K.T. Ng and D.M. Hercules, J. Phys. Chem. **80**, 2094 (1976).
- ⁴²C.K. Jorgensen, Chimia **25**, 213 (1971).
- ⁴³M. Stojanovic, R.G. Haverkamp, C.A. Mims, H. Moudallal, and A.J. Jacobson, J. Catal. **166**, 315 (1997).
- ⁴⁴Z.-J. Kang, L.-P. Li, and Q. Wei, Chem. Res. Chin. Univ. **12**, 280 (1996).
- ⁴⁵E. Talik, A. Novosselov, M. Kulpa, and A. Pajaczkowska, J. Alloys Compd. **321**, 24 (2001).
- ⁴⁶S. Mahl, M. Neumann, G. Borstel, A. Zygmunt, A. Jezierski, and A. Slebarski, J. Magn. Magn. Mater. **159**, 179 (1996).
- ⁴⁷Z. Yang, L. Ye, and X. Xie, Phys. Rev. B **59**, 7051 (1999).
- ⁴⁸Z. Yang, L. Ye, and X. Xie, Phys. Status Solidi B **220**, 885 (2000).